

# The nuclear contacts and short range correlations in nuclei

R. Weiss,<sup>1</sup> R. Cruz-Torres,<sup>2</sup> N. Barnea,<sup>1</sup> E. Piasetzky,<sup>3</sup> and O. Hen<sup>2</sup>

<sup>1</sup>*Racah Institute of Physics, Hebrew University, Jerusalem 91904, Israel*

<sup>2</sup>*Massachusetts Institute of Technology, Cambridge, Massachusetts 02139, USA*

<sup>3</sup>*School of Physics and Astronomy, Tel Aviv University, Tel Aviv 69978, Israel*

(Dated: January 31, 2017)

Atomic nuclei are complex strongly interacting systems and their exact theoretical description is a long-standing challenge. An approximate description of nuclei can be achieved by separating its short and long range structure. This separation of scales stands at the heart of the nuclear shell model and effective field theories that describe the long-range structure of the nucleus using a mean-field approximation. We present here an effective description of the complementary short-range structure using contact terms and stylized two-body asymptotic wave functions. The possibility to extract the nuclear contacts from experimental data is presented. Regions in the two-body momentum distribution dominated by high-momentum, close-proximity, nucleon pairs are identified and compared to experimental data. The amount of short-range correlated (SRC) nucleon pairs is determined and compared to measurements. Non-combinatorial isospin symmetry for SRC pairs is identified. The obtained one-body momentum distributions indicate dominance of SRC pairs above the nuclear Fermi-momentum.

PACS numbers:

## INTRODUCTION:

The atomic nucleus is one of the most complex strongly interacting many-body Fermionic systems in nature. One of the main challenges in describing nuclei is calculating the short-range part of the nuclear wave function. The challenge stems from the complicated nucleon-nucleon interaction and the large density of the nucleus. The latter causes all the relevant scales of the system (size of the nucleons, their average distances, and the range of the interaction) to be comparable, making effective theoretical descriptions very demanding.

Current effective, mean-field, nuclear theories describe well various static properties of nuclei, but fail to describe the dynamic effects of two-nucleon short-range correlation (SRC) pairs, which are a substantial part of the nuclear wave-function. Detailed understanding of such SRCs is important for neutron star structure and the nuclear symmetry energy [1–4], the bound nucleon and free neutron structure functions [5–10], neutrino-nucleus interactions and neutrino oscillation experiments [11–15], and more.

Recent proton and electron scattering experiments indicate that SRC pairs account for 20% - 25% of the nucleons in the nucleus and practically all nucleons with momentum above the Fermi momentum ( $k_F$ ) [16–24]. They are predominantly in the form of neutron-proton (np) SRC pairs with large relative momentum ( $k > k_F$ ), and small center-of-mass (c.m.) momentum ( $K < k_F$ ). Here,  $k_F \sim 250\text{MeV}/c = 1.27\text{fm}^{-1}$  is the typical Fermi momentum of medium and heavy nuclei. Due to their large relative momentum, SRC pairs account for most of the kinetic energy carried by nucleons in the nucleus. These and other results are consistent with the high-momentum ( $k > k_F$ ) tail of the nuclear momentum distribution be-

ing dominated by SRC and described using a factorized wave function for the c.m. and relative momentum distributions of the pairs [25–33]. See recent reviews in [8, 34].

Ab-initio many body calculations of nuclear structure [35–39] are still limited to light nuclei and/or the use of soft interactions that regulate the short-range/high-momentum parts of the nuclear wave function. Effective theories are still needed to describe medium and heavy nuclei and to identify the main physical process at short distances [25–28].

In this work, we study nuclear two-body momentum distributions, obtained from ab-initio many-body calculations. We identify regions dominated by SRC pairs, and compare to experimental data on two-nucleon knockout reactions. We then use the ‘generalized contact formalism’ of Ref. [40] to derive a factorized universal description of SRC in nuclei and determine the nuclear contacts. The contacts obtained separately using two body densities in momentum and coordinate space are consistent. A method to extract the contacts from experimental data is also presented and gives consistent values. The isospin symmetry of SRC pairs is discussed in light of the obtained contacts. Last, we compare the resulting factorized one-body momentum distributions to those derived from many body calculations and confirm the experimental observation that they are dominated by SRC starting from above  $k_F$ .

Momentum and coordinate space densities are a common tool used to study nuclear structure. The one-body momentum densities  $n_N(\mathbf{k})$  define the probability for finding a nucleon with momentum  $\mathbf{k}$ . The two-body densities  $F_{NN}(\mathbf{k}, \mathbf{K})$ , define the probability for finding pair of nucleons with relative momentum  $\mathbf{k}$ , and c.m. momentum  $\mathbf{K}$ . Similarly, the equivalent one- and two-body coordinate space densities,  $\rho_N(\mathbf{r})$  and  $\rho_{NN}(\mathbf{r}, \mathbf{R})$ , define

the probability to find a nucleon at distance  $\mathbf{r}$ , from the c.m. of the nucleus and the probability to find a pair of nucleons with a relative distance  $\mathbf{r}$ , and a c.m. coordinate at distance  $\mathbf{R}$ , from the c.m. of the nucleus. It is also useful to consider the two-body densities integrated over the pair c.m. given by  $F_{NN}(\mathbf{k})$  and  $\rho_{NN}(\mathbf{r})$ . The subscripts N, and NN, stand for the type of nucleon/nucleon-pairs considered (i.e. proton, neutron, proton-proton, neutron-neutron, and proton-neutron).

Recent progress in quantum monte-carlo techniques allows performing ab-initio many-body calculations of nuclear structure for nuclei as heavy as  $^{12}\text{C}$  [35]. These calculations are done using the AV18 and UX, two and three body potentials, and result in one- and two-body nucleon densities in coordinate and momentum space.

Ab-initio many-body calculations of two body densities for nuclei up to  $^{12}\text{C}$  became available only recently [35] and the detailed study of their relation to two-nucleon knockout measurements is only now starting [29, 30, 40].

Two-body densities are a natural tool to study SRCs. However, certain care should be taken to separate high relative momentum SRC pairs from non-correlated pairs with high relative momentum. Nucleons that are part of an SRC pair each have high momentum, their relative momentum is high, and their c.m. momentum is low. Requesting only high relative momentum between nucleons in a pair is not enough to ensure that the individual nucleons have high momentum and therefore are members of SRC pairs.

There are two ways to access regions in the two-body momentum distribution dominated by SRC pairs, with minimal mean-field nucleon contamination. One is to integrate over the pairs c.m. momentum but request a very large relative momentum, which ensures, for any reasonable c.m. momentum, that both individual nucleon momenta are high and that both nucleons truly belong to an SRC pair [40].

The alternative approach is to request pairs with low c.m. momentum and high relative momentum. This approach is equivalent to what is probed experimentally in two-nucleon knockout measurements [20–24], but is more challenging to calculate. To test this approach, we present in Fig. 1, for a variety of nuclei, the ratio of the sum of two-body momentum densities for vanishing c.m. momentum to the one-body proton density  $(2F_{pp}^{K=0}(k) + F_{pn}^{K=0}(k))/n_p(k)$ , where  $F_{NN}^{K=0}(k)$  is the  $K=0$  2-body momentum distribution normalized to the number of NN pairs. We expect this ratio to scale (i.e. be approximately independent of momentum and close to unity) in a region where both the two-body and one-body momentum densities are dominated by SRC pairs [40]. As can be seen, scaling is observed starting at  $k_F$ . This is an indication, coming from ab-initio calculations, that the one-body momentum distribution, starting at  $k_F$ , is dominated by SRC pairs, as observed experimentally [16–24].

How well requiring low c.m. momentum and high relative momentum selects SRC pairs can be studied by comparing the two-body density calculations to data. Fig. 2 shows the calculated and measured proton-proton (pp) to proton-neutron (pn) pairs density ratios in  $^4\text{He}$  as a function of their relative momentum. The experimental data are obtained from recent electron induced two-nucleon knockout measurements performed in kinematics dominated by breakup of SRC pairs [23]. The calculated pair density ratio is shown as a function of the relative pair momentum and is given by:  $\int_0^{K_{max}} d\mathbf{K} F_{pp}(\mathbf{k}, \mathbf{K}) / \int_0^{K_{max}} d\mathbf{K} F_{pn}(\mathbf{k}, \mathbf{K})$ , where  $K_{max}$  varies from zero to infinity. As can be seen, the calculated ratio, is insensitive to the c.m. momentum integration up to 1 - 1.5  $\text{fm}^{-1}$  (i.e.  $K_{max} \sim k_F$ ). Higher c.m. momentum significantly affects the ratio at relative momenta of about 1.5 - 2.5  $\text{fm}^{-1}$  and is becoming inconsistent with the experimental data. These results are inline with those of Ref. [29]. One should note that at very high relative momentum the ratio is insensitive to the c.m. integration, as expected.

Studies of dilute Fermi systems have showed that if the interaction range  $r_0$  is much shorter than the average interparticle distance  $d$ , and the scattering length  $a_s$ , a contact theory can be used to describe the system [41–44]. A series of relations between different observables and the probability of finding a particle pair in close proximity emerge. The basis of the contact theory lays with the significant separation of scales in the system. This allows using the Bethe-Peierls boundary condition that leads to a factorized asymptotic wave-function at short distances of the form [44]:

$$\Psi \xrightarrow{r_{ij} \rightarrow 0} \varphi(\mathbf{r}_{ij}) A_{ij}(\mathbf{R}_{ij}, \{\mathbf{r}\}_{k \neq ij}), \quad (1)$$

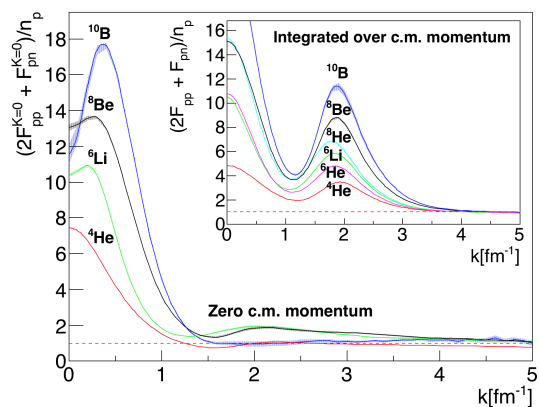


FIG. 1: The ratio of the calculated sum of two-body momentum densities (2 proton-proton + proton-neutron pairs) to the one-body proton density, as a function of the relative momentum. The momentum densities are taken from Ref. [35], where the two-body densities have vanishing pair c.m. momentum. The insert, taken from Ref. [40], are for two-body densities integrated over the pair c.m. momentum.

where  $\varphi(\mathbf{r}_{ij})$  is a two-body wave function and  $A_{ij}$  is a function of the residual  $A - 2$  particles system. The scale separation allows replacing the short-range interaction with a boundary condition such that  $\varphi(\mathbf{r}_{ij}) = (1/r_{ij} - 1/a_s)$ . In momentum space, this factorized wave function leads to a high momentum tail for  $|a_s|^{-1}, d^{-1} \ll k \ll r_0^{-1}$  that is given by:  $n(k) \rightarrow C/k^4$ , where  $C = 16\pi^2 \sum_{ij} \langle A_{ij} | A_{ij} \rangle$  is known as the contact.

The contact theory was studied in great detail theoretically, and validated experimentally, for ultra-cold fermi gases [41–51]. For nuclei, several experimental observations resemble those of cold atomic systems [52, 53]. However, the theoretical basis for this comparison is unclear, since the required scale separation does not strictly apply for nuclear systems.

In nuclei, all relevant scales are comparable. The short-range interaction is about 0.5-1 fm, the average distance between nucleons is about 2 fm, and the scattering length is about -20 fm and 5 fm for the triplet and singlet channels respectively. The small difference between the interaction range and the average density sets the predicted scaling region to be below  $k_F$ .

To better understand the experimental observations, Ref. [40] proposed a generalized contact theory for nuclei. The generalization has two main parts: (1) a sum over all possible nucleon-nucleon channels and (2) the use of a general two-body wave-function that solves the nuclear zero-energy two-body problem. In this generalized formalism, the independent pair approximation [54] is used to express the factorized asymptotic wave-function

(Eq. 1) as:

$$\Psi \xrightarrow{r_{ij} \rightarrow 0} \sum_{\alpha} \varphi_{\alpha}(\mathbf{r}_{ij}) A_{ij}^{\alpha}(\mathbf{R}_{ij}, \{\mathbf{r}\}_{k \neq ij}) \quad (2)$$

where the sum over  $\alpha$  spans all the possible two-body states of the nucleon-nucleon pairs and the index  $ij$  corresponds to  $pn$ ,  $pp$ , and  $nn$  pairs [58].

In the following, we will consider only the main channels contributing to SRCs, namely, the  $pn$  deuteron channel ( $\ell = 0, 2$  and  $s = 1$  coupled to  $j = 1$ ) and the singlet  $s$ -wave channel ( $\ell = s = j = 0$ ).

Using Eq. (2), asymptotic expressions for the one- and two-body momentum densities can be derived [40]:

$$n_p(\mathbf{k}) = 2C_{pp}^{s=0} |\tilde{\varphi}_{pp}^{s=0}(\mathbf{k})|^2 + C_{pn}^{s=0} |\tilde{\varphi}_{pn}^{s=0}(\mathbf{k})|^2 + C_{pn}^{s=1} |\tilde{\varphi}_{pn}^{s=1}(\mathbf{k})|^2 \quad (3)$$

$$F_{pp}(\mathbf{k}) = C_{pp}^{s=0} |\tilde{\varphi}_{pp}^{s=0}(\mathbf{k})|^2 \\ F_{pn}(\mathbf{k}) = C_{pn}^{s=0} |\tilde{\varphi}_{pn}^{s=0}(\mathbf{k})|^2 + C_{pn}^{s=1} |\tilde{\varphi}_{pn}^{s=1}(\mathbf{k})|^2 \quad (4)$$

and the same when replacing  $n$  with  $p$ . Here,  $C_{ij}^{\alpha}$  are the nuclear contacts that determine the number of pairs in a given two-body channel. Clearly,  $n_{p(n)}(\mathbf{k}) = 2F_{pp(nn)}(\mathbf{k}) + F_{pn}(\mathbf{k})$  [40]. Equivalent two-body coordinate space densities for  $\rho_{NN}(\mathbf{r})$  are given by replacing  $\tilde{\varphi}(\mathbf{k})$  with  $\varphi(\mathbf{r})$  in Eq. (4). We note that deriving the one-body momentum relation from Eq. (3), the center-of-mass momentum of the pairs was assumed to be much smaller than  $k$ .

We choose to normalize  $\tilde{\varphi}(\mathbf{k})$  such that  $\int_{k_F}^{\infty} |\tilde{\varphi}(\mathbf{k})|^2 d\mathbf{k} = 1$  for  $k_F = 250 \text{ MeV}/c = 1.27 \text{ fm}^{-1}$ . Using this normalization, and Eq. (3), the fraction of the one-body momentum density above  $k_F$  is given by:

$$\frac{\int_{k_F}^{\infty} n(\mathbf{k}) d\mathbf{k}}{\int_0^{\infty} n(\mathbf{k}) d\mathbf{k}} = \frac{C_{nn}^{s=0} + C_{pp}^{s=0} + C_{pn}^{s=0} + C_{pn}^{s=1}}{A/2}, \quad (5)$$

where  $n(\mathbf{k}) = n_n(\mathbf{k}) + n_p(\mathbf{k})$ ,  $A$  is the number of nucleons in the nucleus  $C_{NN}^s/(A/2)$  gives the fraction of the one-body momentum density above the Fermi momentum due to each type of SRC pair.

As explained above, we consider four main nuclear contacts: singlet  $\ell = 0$   $pn$ ,  $pp$ , and  $nn$ , and triplet  $pn$  deuteron channel. For symmetric nuclei, spin-zero  $pp$  and  $nn$  pairs are identical, leaving three nuclear contacts:  $C_{nn}^{s=0}$ ,  $C_{pn}^{s=0}$ , and  $C_{pn}^{s=1}$ . Isospin symmetry can be used to relate the various  $s = 0$  contacts, leaving two independent contacts: spin-singlet and spin-triplet. For what follows, we do not impose isospin symmetry in order to study its manifestation in the case of SRC pairs.

The value of the contacts, extracted by fitting the factorized two-body momentum (coordinate) space expressions of Eq. (4) to the equivalent two-body density obtained from many-body variational monte-carlo (VMC)

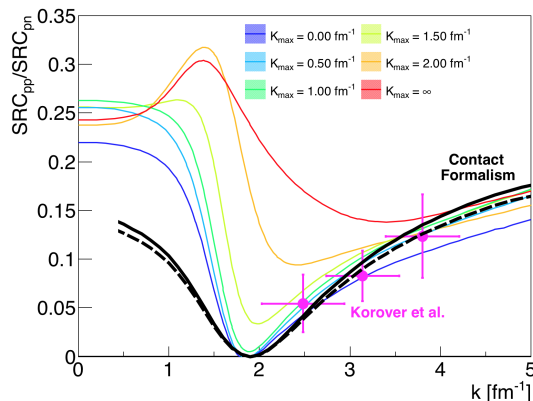


FIG. 2: The ratio of proton-proton to proton-neutron SRC pairs in  ${}^4\text{He}$  as a function of the pair momentum extracted from  ${}^4\text{He}(e,e'pN)$  measurements [23]. The colored lines show the equivalent ab-initio two-body momentum densities ratio integrated over the c.m. momentum from 0 to  $K_{max}$  that varies from zero to infinity [35]. The solid (dashed) black line is the ratio of the two-body momentum densities calculated using the contact formalism with the contacts extracted in momentum (coordinate) space (Eq. (7)).

calculations [35], are listed in Table I for a variety of nuclei. The  $s = 0$   $pp$  and  $nn$  contacts are obtained by fitting the VMC  $pp$  and  $nn$  two-body density respectively. The  $s = 1$  and  $s = 0$   $pn$  contacts are obtained from simultaneously fitting the spin=1 isospin=0  $pn$  two-body density and the total  $pn$  two-body density. The fitting range was  $4 \text{ fm}^{-1}$  to  $4.8 \text{ fm}^{-1}$ . The uncertainty of the resulting contacts is obtained by varying the fit limits by  $\pm 0.2 \text{ fm}^{-1}$  [58].

Table I also lists the nuclear contacts obtained by fitting the two-body coordinate space density in the range of  $0.25 \text{ fm}$  to  $1 \text{ fm}$ . The uncertainties are obtained by varying the fit limits by  $\pm 0.25 \text{ fm}$ . As VMC coordinate space distributions are not available for the different spin-isospin states, we assumed isospin symmetry (i.e. equal  $s = 0$  contacts) for the symmetric nuclei.

The contacts extracted separately by fitting the high-momentum and short-distance two-body densities are consistent. This points to a quantitative equivalence between high-momentum and short-range physics in nuclear systems. Another interesting feature is that, for symmetric nuclei, the momentum space  $s = 0$   $pp$  and  $pn$  contacts are the same within uncertainties, in contrast to combinatorial expectations.

Fig. 3 compares the  ${}^4\text{He}$  one-body momentum distribution obtained from many-body VMC calculations to the prediction of the nuclear contact theory, Eq. (3). Also shown are the contributions of the various channels to the total momentum distribution and the ratio of the VMC calculation to Eq. (3). As can be seen, the asymptotic 1-body density, as predicted by the contact theory, reproduces with 10% accuracy the many-body calculation starting from  $k_F$  to  $5 \text{ fm}^{-1}$ , where the momentum density varies over 4 orders of magnitude. Similar comparisons for other nuclei listed in Table I show a similar 10% - 20% agreement for  $k_F \leq k \leq 5 \text{ fm}^{-1}$  [58].

The contacts can also be used to calculate the  $pp$  to  $pn$  SRC pairs ratio. This ratio can be compared with experimental electron induced two-nucleon knockout data [20–24]. The data and the contact theory predictions are shown for  ${}^4\text{He}$  in Fig. 2. A similar comparison for  ${}^{12}\text{C}$  [22] also shows a good agreement [58].

Experimentally, the nuclear contacts can be evaluated using the measured  $pp$ -to- $pn$  SRC pairs ratio,  $\frac{SRC_{pp}}{SRC_{pn}}(k)$ , and the high-momentum scaling factor,  $a_2(A/d)$ . The latter is extracted from inclusive electron scattering cross-section ratios and determines the relative number of high-momentum ( $k > k_F$ ) nucleons in a nucleus,  $A$ , relative to deuterium [9, 16–19]. Within the contact formalism, these experimental quantities can be expressed as:

$$a_2(A/d) \int_{k_F}^{\infty} |\tilde{\psi}_d(\mathbf{k})|^2 d\mathbf{k} = \frac{C_{nn}^{s=0} + C_{pp}^{s=0} + C_{pn}^{s=0} + C_{pn}^{s=1}}{A/2} \quad (6)$$

$$\frac{SRC_{pp}}{SRC_{pn}}(k) = \frac{C_{pp}^{s=0} |\tilde{\varphi}_{pp(nn)}^{s=0}(k)|^2}{C_{pn}^{s=0} |\tilde{\varphi}_{pn}^{s=0}(k)|^2 + C_{pn}^{s=1} |\tilde{\varphi}_{pn}^{s=1}(k)|^2} \quad (7)$$

where  $\tilde{\psi}_d(\mathbf{k})$  is deuteron wave function, normalized to one. The relation of the  $pp$ -to- $pn$  SRC pairs ratio to the nuclear contacts assumes that the c.m. motion of SRC pairs is small, and similar for the different types of SRC pairs in a given nucleus, as observed experimentally [22–24, 55]. For symmetric nuclei, assuming isospin symmetry, we can solve Eq. (6) and Eq. (7), and express the  $s = 0, 1$  contacts as a function of the measured quantities and the universal functions. The contacts extracted using this method for  ${}^4\text{He}$  and  ${}^{12}\text{C}$ , listed in Table I, are consistent with those extracted from the VMC many-body calculations.

According to our analysis, the contribution of correlated pairs in the spin-isospin  $ST = 11$  channel to the one-body momentum density for  $k > k_F$  is very small. The fact that the contact formalism reproduces the VMC one-body momentum density to 10% - 20% accuracy, without utilizing the  $ST = 11$  channel, indicates its small importance for the nuclei considered here. This stands in contrast to other works that do find a non-negligible contribution of  $ST = 11$  pairs [56, 57]. A possible explanation for this difference can be attributed to contributions from un-correlation pairs in the  $ST = 11$  channel. Specifically, Alvioli et al., obtained the one-body momentum

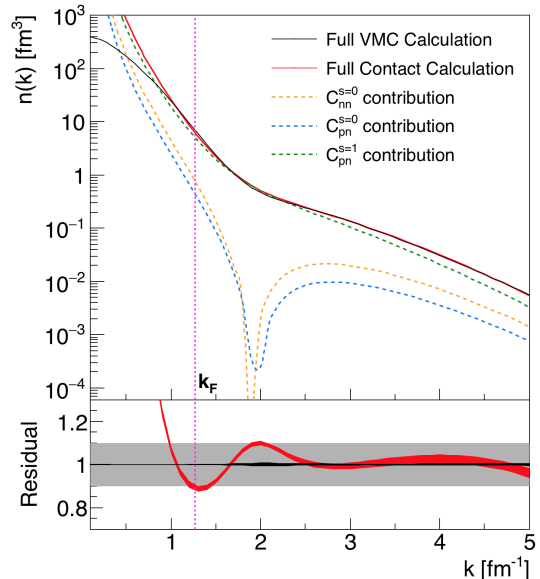


FIG. 3:  ${}^4\text{He}$  one-body momentum density extracted from ab-initio VMC calculations (solid black band) and using the nuclear contact formalism (solid red band). The dashed lines show the contribution of different channels to the total contact calculation, using the contacts extracted in momentum space. The residual plot shows the ratio of the contact calculations to the VMC. The shaded region marks the 10% agreement region. The width of the black and red lines represents the individual uncertainties in the calculations.

TABLE I: The nuclear contacts for a variety of nuclei. The contacts are extracted by fitting the asymptotic expressions of Eq. (4) to the VMC two-body densities in momentum ( $k$ ) and coordinate ( $r$ ) space separately. For  ${}^4\text{He}$  and  ${}^{12}\text{C}$  the contacts extracted from electron scattering data are also shown. The nuclear contacts are divided by  $A/2$  and multiplied by 100 to give the percent of nucleons above  $k_F$  given by the different SRC pairs.

A	k-space				r-space			
	$C_{pn}^{s=1}$	$C_{pn}^{s=0}$	$C_{nn}^{s=0}$	$C_{pp}^{s=0}$	$C_{pn}^{s=1}$	$C_{pn}^{s=0}$	$C_{nn}^{s=0}$	$C_{pp}^{s=0}$
${}^4\text{He}$	$12.3 \pm 0.1$	$0.69 \pm 0.03$	$0.65 \pm 0.03$		$11.61 \pm 0.03$	$0.567 \pm 0.004$		
	$14.9 \pm 0.7$ (exp)	$0.8 \pm 0.2$ (exp)						
${}^6\text{Li}$	$10.5 \pm 0.1$	$0.53 \pm 0.05$	$0.49 \pm 0.03$		$10.14 \pm 0.04$	$0.415 \pm 0.004$		
${}^7\text{Li}$	$10.6 \pm 0.1$	$0.71 \pm 0.06$	$0.78 \pm 0.04$	$0.44 \pm 0.03$	$9.0 \pm 2.0$	$0.6 \pm 0.4$	$0.647 \pm 0.004$	$0.350 \pm 0.004$
${}^8\text{Be}$	$13.2 \pm 0.2$	$0.86 \pm 0.09$	$0.79 \pm 0.07$		$12.0 \pm 0.1$	$0.603 \pm 0.003$		
${}^9\text{Be}$	$12.3 \pm 0.2$	$0.90 \pm 0.10$	$0.84 \pm 0.07$	$0.69 \pm 0.06$	$10.0 \pm 3.0$	$0.7 \pm 0.7$	$0.65 \pm 0.02$	$0.524 \pm 0.005$
${}^{10}\text{B}$	$11.7 \pm 0.2$	$0.89 \pm 0.09$	$0.79 \pm 0.06$		$10.7 \pm 0.2$	$0.57 \pm 0.02$		
${}^{12}\text{C}$	$16.8 \pm 0.8$	$1.4 \pm 0.2$	$1.3 \pm 0.2$		$14.9 \pm 0.1$	$0.83 \pm 0.01$		
	$18 \pm 2$ (exp)	$1.5 \pm 0.5$ (exp)						

density by integrating the two-body momentum density without limiting the c.m. momentum of the pairs, possibly allowing for contributions from non-correlated pairs.

Even though nuclear systems do not strictly fulfill the scale-separation conditions required by the contact theory, both the ab-initio one body momentum distribution above  $k_F$  and the experimental data are well reproduced using factorized asymptotic wave-functions and nuclear contact theory.

Consistent contacts extracted by separately fitting coordinate and momentum space two-body densities show equivalence between high-momentum and short-range dynamics in nuclear systems. The values of the contacts in the spin-zero channels reveal the non-combinatorial isospin-spin symmetry of SRCs.

This work complements previous works discussing the factorization of the nuclear momentum density in momentum space using effective calculations [25–29], extending the discussion to coordinate space densities and relating them in a global formalism of generalized contact theory. Future work will study the applicability of the contact formalism to describe the nuclear spectral function, correlation function, and more.

We would like to thank B. Bazak, W. Cosyn, C. Degli-Atti, S. Gandolfi, G. Miller, E. Pazi, J. Ryckebush, M. Sargsian, M. Strikman, and L.B. Weinstein for many fruitful discussions. This work was supported by the Pazy foundation, the Israel Science Foundation (grant no. 136/12, and 1334/16), and the U.S. Department of Energy Office of Science, Office of Basic Energy Sciences program under award number DE-FG02-94ER40818.

[1] L. Frankfurt, M. Sargsian, and M. Strikman, International Journal of Modern Physics A **23**, 2991 (2008).  
[2] O. Hen, B.-A. Li, W.-J. Guo, L. B. Weinstein, and E. Pi-

asetzky, Phys. Rev. C **91**, 025803 (2015), URL <http://link.aps.org/doi/10.1103/PhysRevC.91.025803>.  
[3] B.-J. Cai and B.-A. Li, Phys. Rev. **C93**, 014619 (2016), 1509.09290.  
[4] O. Hen, A. W. Steiner, E. Piasetzky, and L. B. Weinstein (2016), 1608.00487.  
[5] L. B. Weinstein, E. Piasetzky, D. W. Higinbotham, J. Gomez, O. Hen, and R. Shneor, Phys. Rev. Lett. **106**, 052301 (2011).  
[6] O. Hen, A. Accardi, W. Melnitchouk, and E. Piasetzky, Phys. Rev. D **84**, 117501 (2011), URL <http://link.aps.org/doi/10.1103/PhysRevD.84.117501>.  
[7] O. Hen, D. W. Higinbotham, G. A. Miller, E. Piasetzky, and L. B. Weinstein, Int. J. Mod. Phys. **E22**, 1330017 (2013), 1304.2813.  
[8] O. Hen, G. A. Miller, E. Piasetzky, and L. B. Weinstein (2016), 1611.09748.  
[9] O. Hen, E. Piasetzky, and L. B. Weinstein, Phys. Rev. C **85**, 047301 (2012).  
[10] J.-W. Chen, W. Detmold, J. E. Lynn, and A. Schwenk (2016), 1607.03065.  
[11] H. Gallagher, G. Garvey, and G. P. Zeller, Ann. Rev. Nucl. Part. Sci. **61**, 355 (2011).  
[12] L. Fields et al. (MINERvA Collaboration), Phys. Rev. Lett. **111**, 022501 (2013), URL <http://link.aps.org/doi/10.1103/PhysRevLett.111.022501>.  
[13] G. A. Fiorentini et al. (MINERvA Collaboration), Phys. Rev. Lett. **111**, 022502 (2013).  
[14] R. Acciarri et al., Phys. Rev. D **90**, 012008 (2014), URL <http://link.aps.org/doi/10.1103/PhysRevD.90.012008>.  
[15] L. B. Weinstein, O. Hen, and E. Piasetzky, Phys. Rev. **C94**, 045501 (2016), 1604.02482.  
[16] L. Frankfurt, M. Strikman, D. Day, and M. Sargsyan, Phys. Rev. C **48**, 2451 (1993).  
[17] K. Egiyan et al. (CLAS Collaboration), Phys. Rev. C **68**, 014313 (2003).  
[18] K. Egiyan et al. (CLAS Collaboration), Phys. Rev. Lett. **96**, 082501 (2006).  
[19] N. Fomin et al., Phys. Rev. Lett. **108**, 092502 (2012).  
[20] A. Tang et al., Phys. Rev. Lett. **90**, 042301 (2003).  
[21] E. Piasetzky, M. Sargsian, L. Frankfurt, M. Strikman, and J. W. Watson, Phys. Rev. Lett. **97**, 162504 (2006).

- [22] R. Subedi et al., *Science* **320**, 1476 (2008).
- [23] I. Korover, N. Muangma, O. Hen, et al., *Phys.Rev.Lett.* **113**, 022501 (2014), 1401.6138.
- [24] O. Hen et al. (CLAS Collaboration), *Science* **346**, 614 (2014).
- [25] J. Ryckebusch, M. Vanhalst, and W. Cosyn, *Journal of Physics G: Nuclear and Particle Physics* **42**, 055104 (2015), URL <http://stacks.iop.org/0954-3899/42/i=5/a=055104>.
- [26] M. Vanhalst, J. Ryckebusch, and W. Cosyn, *Phys. Rev. C* **86**, 044619 (2012).
- [27] C. Colle et al., *Phys. Rev. C* **92**, 024604 (2015).
- [28] C. Ciofi degli Atti and S. Simula, *Phys. Rev. C* **53**, 1689 (1996), nucl-th/9507024.
- [29] M. Alvioli, C. Ciofi degli Atti, and H. Morita, *Phys. Rev. C* **94**, 044309 (2016), 1607.04103.
- [30] M. Alvioli, C. Ciofi Degli Atti, L. P. Kaptari, C. B. Mezzetti, and H. Morita, *Int. J. Mod. Phys. E* **22**, 1330021 (2013), 1306.6235.
- [31] T. Neff, H. Feldmeier, and W. Horiuchi, *Phys. Rev. C* **92**, 024003 (2015), URL <http://link.aps.org/doi/10.1103/PhysRevC.92.024003>.
- [32] L. L. Frankfurt and M. I. Strikman, *Phys. Rep.* **76**, 215 (1981).
- [33] L. Frankfurt and M. Strikman, *Phys. Rep.* **160**, 235 (1988).
- [34] C. Ciofi degli Atti, *Phys. Rept.* **590**, 1 (2015).
- [35] R. B. Wiringa, R. Schiavilla, S. C. Pieper, and J. Carlson, *Phys. Rev. C* **89**, 024305 (2014).
- [36] J. Carlson, S. Gandolfi, F. Pederiva, S. C. Pieper, R. Schiavilla, K. E. Schmidt, and R. B. Wiringa, *Rev. Mod. Phys.* **87**, 1067 (2015), 1412.3081.
- [37] G. Hagen et al., *Nature Phys.* **12**, 186 (2015), 1509.07169.
- [38] A. Rios, A. Polls, and W. H. Dickhoff, *Phys. Rev. C* **79**, 064308 (2009), 0904.2183.
- [39] A. Rios, A. Polls, and W. H. Dickhoff, *Phys. Rev. C* **89**, 044303 (2014), 1312.7307.
- [40] R. Weiss, B. Bazak, and N. Barnea, *Phys. Rev. C* **92**, 054311 (2015), 1503.07047.
- [41] S. Tan, *Annals of Physics* **323**, 2952 (2008).
- [42] S. Tan, *Annals of Physics* **323**, 2971 (2008).
- [43] S. Tan, *Annals of Physics* **323**, 2987 (2008).
- [44] E. Braaten, in *The BCS-BEC Crossover and the Unitary Fermi Gas*, edited by W. Zwerger (Springer, Berlin, 2012).
- [45] S. Gandolfi, K. E. Schmidt, and J. Carlson, *Phys. Rev. A* **83**, 041601 (2011).
- [46] J. T. Stewart, J. P. Gaebler, T. E. Drake, and D. S. Jin, *Phys. Rev. Lett.* **104**, 235301 (2010).
- [47] E. D. Kuhnle, H. Hu, X.-J. Liu, P. Dyke, M. Mark, P. D. Drummond, P. Hannaford, and C. J. Vale, *Phys. Rev. Lett.* **105**, 070402 (2010).
- [48] G. Partridge, K. Strecker, R. Kamar, M. Jack, and R. Hulet, *Phys. Rev. Lett.* **95**, 020404 (2005).
- [49] F. Werner, L. Tarruell, and Y. Castin, *The European Physical Journal B* **68**, 401 (2009), ISSN 1434-6028.
- [50] A. Schirotzek, Ph.D. thesis, Massachusetts Institute of Technology (2010).
- [51] Y. Sagi, T. Drake, R. Paudel, and D. Jin, *Phys. Rev. Lett.* **109**, 220402 (2012).
- [52] O. Hen, L. B. Weinstein, E. Piasetzky, G. A. Miller, M. M. Sargsian, and Y. Sagi, *Phys. Rev. C* **92**, 045205 (2015), URL <http://link.aps.org/doi/10.1103/PhysRevC.92.045205>.
- [53] R. Weiss, B. Bazak, and N. Barnea, *Phys. Rev. Lett.* **114**, 012501 (2015).
- [54] L. C. Gomes, J. D. Walecka, and V. F. Weisskopf, *Annals Phys.* **3**, 241 (1958).
- [55] R. Shneor et al., *Phys. Rev. Lett.* **99**, 072501 (2007).
- [56] H. Feldmeier, W. Horiuchi, T. Neff, and Y. Suzuki, *Phys. Rev. C* **84**, 054003 (2011), 1107.4956.
- [57] M. Alvioli, C. Ciofi degli Atti, L. P. Kaptari, C. B. Mezzetti, and H. Morita, *Phys. Rev. C* **87**, 034603 (2013), 1211.0134.
- [58] . Online supplementary materials (2016).